Glycobiology vol. 20 no. 2 pp. 166–174, 2010
doi:10.1093/glycob/cwp158
Advance Access publication on October 20, 2009

Comparison of the substrate specificities and catalytic properties of the sister *N*-acetylglucosaminyltransferases, GnT-V and GnT-Vb (IX)

Gerardo Alvarez-Manilla[3], Karolyn Troupe[2], Maria Fleming[2], Erika Martinez-Uribe[2], and Michael Pierce[1,2]

[2]Department of Biochemistry and Molecular Biology, Complex Carbohydrate Research Center, University of Georgia, Athens, GA 30602; and [3]Ezose Sciences Inc. Pine Brook, NJ, 07058, USA

Received on February 12, 2009; revised on September 24, 2009; accepted on September 27, 2009

***N*-Acetylglucosaminlyltransferase-V (GnT-V) synthesizes GlcNAcβ1,6Man branched *N*-glycans both in vitro and in vivo. A paralog, GnT-Vb (or GnT-IX), has also been shown to synthesize both GlcNAcβ1,6Man branched *N*- and *O*-glycans. GnT-V is expressed in most human and rodent tissues while GnT-Vb expression is limited mainly to neural tissue and testes. It is of interest, therefore, to compare the catalytic properties and reaction kinetics of these sister enzymes. The results demonstrate that while GnT-V was fully active without exogenous cation and in the presence of EDTA, the activity of GnT-Vb was stimulated over 4-fold in the presence of 10 mM Mn^{++}. The pH optimum for GnT-V was in the range of 6.5–7.0, while that of GnT-Vb was 8.0. common for glycosyltransferases active in brain. Both enzymes transferred GlcNAcβ1,6 to the Man residue of the GlcNAcβ1,2Man moiety of glycan substrates, and both enzymes acted effectively on a synthetic GlcNAcβ1,2Manα1,2Glc-*O*-octyl trisaccharide acceptor. Moreover, although both enzymes utilized an *N*-linked asialo-agalacto-biantennary glycan as an acceptor, GnT-Vb displayed an almost 2.5-fold higher apparent K_m value compared to GnT-V. Conversely, GnT-Vb very efficiently glycosylated a synthetic glycopeptide, Ac-H_2N-Val-Glu-Pro-(GlcNAcβ1,2-Man-*O*-)Thr-Ala-Val-CO-Ac, while GnT-V showed relatively poor activity toward this *O*-Man-linked glycopeptide acceptor, with a K_m value of 20-fold higher than that of GnT-Vb. When the *N*-linked asialo-agalacto-biantennary glycan acceptor was utilized with GnT-Vb, the expected triantennary β1,6-branched product was observed up to 8 h incubation. An additional product with two β1,6-linked GlcNAc resides, however, was observed after prolonged (>8 h) incubation, consistent with an earlier report. This unusual tetraantennary product was observed with GnT-Vb only after substantial accumulation of the first triantennary product and not during the early stages of incubation.**

Keywords: beta-1,6-Glucosaminyltransferase Vb/GnT-Vb/GnT-IX/Peptide O-Mannosyl beta-1,2-Glicosaminyltransferase I (POMGnT-I)/Glycosyltransferase/Glycopeptides/Kinetics

[1]To whom correspondence should be addressed: Tel: +1-706-542-1702; Fax: +1-706-542-1769; e-mail: Hawkeye@uga.edu

Introduction

N-Acetylglucosaminyltransferase V (GnT-V) catalyzes transfer of GlcNAc in β(1,6)-linkage to the α(1,6)-linked mannose in bi- and tri-antennary *N*-linked glycans. Genomic sequences encoding the enzyme have been identified in animals ranging from *C. elegans* to man (Shoreibah et al. 1993; Saito et al. 1994; Warren et al. 2002). The rodent and human enzymes differ by only one amino acid out of 814, demonstrating extremely strong sequence conservation. GnT-V is expressed in most human cell types, but its glycan product, often detected by the binding L-phytohemagglutinin (L-PHA), is not observed in mature breast and colorectal epithelia (Fernandes et al. 1991). Increased expression of GnT-V products has been observed in many, but not all, oncogenically transformed cell types, and in the case of breast and colorectal carcinomas, the products are associated with invasiveness and poor prognosis (Zhao, Sato, et al. 2008; Zhao, Takahashi, et al. 2008). GnT-V transcript expression can be regulated by the *ras-ets* signaling pathway, as well as others, and oncogene activation that affects these pathways leads to overexpression of the enzyme and its glycan products (Kang et al. 1996; Buckhaults et al. 1997). The clustering and signaling of cell surface adhesion receptors, including several integrin subunits, N- and E-cadherin, as well as the endocytosis and signaling of the epidermal growth factor receptor, have been shown to be significantly affected by changes in GnT-V expression (Partridge et al. 2004; Guo et al. 2007; Zhao, Sato, et al. 2008). Some of these effects have been postulated to involve galectin–glycan ligand interactions on the cell surface, regulating surface residency times and intracellular signaling (Partridge et al. 2004).

A sister enzyme of GnT-V has been described by two groups (Inamori et al. 2003; Kaneko et al. 2003; Kim et al. 2006), designated GnT-IX and GnT-Vb, respectively. In vitro, the enzyme can synthesize the β(1,6)-GlcNAc linkage to the α(1,6)-linked Man on *N*-linked glycans, identically to the GnT-V reaction. Moreover, transient expression of GnT-Vb in Lec4 CHO cells that lack functional GnT-V activity and L-PHA binding glycans resulted in expression of glycans on the surfaces of Lec4 that bound L-PHA at near wild-type CHO cell levels (Kaneko et al. 2003). In addition, using recombinant GnT-Vb purified from cell extracts and a lengthy incubation with an *N*-linked agalacto-biantennary glycan, an additional product was identified by NMR spectroscopy (Inamori et al. 2003). In this unusual product, GlcNAc was also added to the α1,3-linked Man in a β1,6-linkage, synthesizing a tetraantennary structure with a GlcNAc residue linked β(1,6) to each of the alpha-linked Man

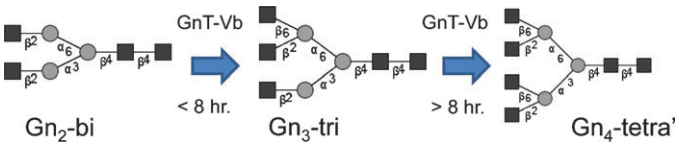

Scheme I. GlcNAc addition to the asialo-agalacto biantennary glycan substrate catalyzed in vitro by GnTVb.

residues, a unique glycan structure not previously reported (see Scheme I). Primarily because of the appearance of this unusual structure, the enzyme was termed GnT-IX by Inamori et al. These experiments demonstrated in vivo and in vitro that GnT-Vb could synthesize *N*-linked glycans with GlcNAc β1,6 branches. Subsequently, GnT-Vb (GnT-IX) was convincingly shown to synthesize in vitro the GlcNAc β1,6 branch on an *O*-Man-linked glycan, GlcNAcβ1,2-(**GlcNAcβ1,6**)Manα1-Ser-(Inamori et al. 2004). This product, however, was not observed when GnT-V was incubated with the same substrate under the same reaction conditions. The relative abilities of the enzyme to transfer to *N*-linked versus *O*-linked structures were not reported, however.

Glycans linked to Ser/Thr through an *O*-linked Man residue have been known in fungi for many years (e.g., Lehle et al. (1979)). Their description and quantitation in mammals, however, has only occurred relatively recently (Yuen et al. 1997; Chai et al. 1999). Quantitation of the levels of *O*-Man glycans relative to *O*-GalNAc glycans in rabbit brain yielded a ratio of about 1:4, respectively, a significant level for a type of glycan not recognized for many years to occur in mammalian tissues. Also described in rabbit brain were *O*-Man-linked glycans containing a β(1,6)branch, constituting a significant amount of the *O*-Man structures in this tissue. In muscle, however, glycans with this branch do not appear to be expressed at significant levels (Endo and Manya 2006). The non-branched *O*-Man glycan in muscle, expressed predominantly on α-dystroglycan, is clearly essential for nerve–muscle adhesion since mutations in the glycosyltransferases that synthesize this glycan cause several human disorders with phenotypes of muscular dystrophy (Schachter et al. 2004; Endo 2005). In brain, expression of glycosyltransferases with these mutations results in aberrant neuronal migration. GnT-Vb endogenously expressed in mouse brain is active toward an asialo-agalacto-biantennary *N*-linked glycan, and mice that lack GnT-V express active GnT-Vb (IX) (Inamori et al. 2006), confirming the results of Kaneko et al. (2003) using Lec4 CHO cells that GnT-Vb activity is not dependent on expression of functional Va. The function of GnT-Vb in brain neural tissue is not as yet understood.

GnT-V and Vb show high degrees of amino acid sequence identity and similarity, particularly in their catalytic regions. Knowledge of the details of their acceptor specificities and kinetic properties, therefore, is an important first step to understand the function of these enzymes, particularly in neural tissue where they are both expressed during development and in the adult. To this end, we have studied the catalytic properties of recombinant GnT-Vb in vitro, including cation stimulation and pH optima, determined the K_m values of the reaction of the enzyme with several *N*- and *O*-linked glycan substrates, and characterized the structures of some of the products, comparing these results with those obtained using GnT-V.

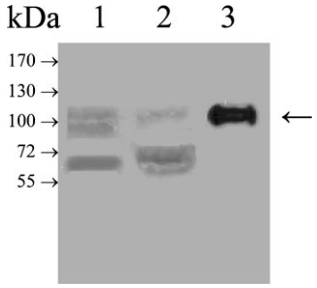

Fig. 1. Western blot detection of partially purified recombinant GnT-Vb from HEK-293 cells using an anti-His antibody. A cDNA encoding recombinant, secreted form of GnT-Vb with an N-terminal 6-His tag was transfected into HEK-293 cells, and the enzyme secreted into the media was partially purified using a nickel-chelating column (as described in *Material and methods*). Lane 1, total cell lysate; lane 2, culture media; lane 3, concentrate after nickel chelating column chromatography.

Results

In order to gain insights into the acceptor specificities of GnT-V and Vb, a recombinant, soluble form of GnT-Vb without its N-terminal transmembrane domain but with a signal secretion sequence and an N-terminal His_6 tag for purification was constructed and stably expressed in HEK-293 cells using the pEAK vector system. EST human and mouse databases display two forms of GnT-Vb, one that is two amino acids longer and is likely due to a variation in transcriptional splicing (Kaneko et al. 2003). A cDNA encoding the short form of the enzyme shown to be active when transiently expressed was constructed and expressed in HEK-293 cells. Western blot analysis using a mouse monoclonal antibody against the His_6 tag showed in cell lysates and cell supernatants, a protein band at about 100 kDa, close to the predicted molecular weight of 90 kDa (Figure 1, lanes 1 and 2). Purification by nickel column chromatography of the secreted enzyme revealed a band at about 100 kDa by Western blotting with the anti-His_6 antibody (Figure 1, lane 3). Analysis of this enzyme preparation by SDS–PAGE revealed the presence of other protein bands (data not shown). Activity assays of the HEK-293 culture media with the GlcNAcβ1-2Manα1-2Glc-*O*-octyl acceptor and UDP-[^{3}H]-GlcNAc (Palcic et al. 1988) revealed abundant activity, and this partially purified preparation was used for subsequent experiments since no interfering hydrolase activities could be detected.

Using the synthetic trisaccharide acceptor, assay conditions were adjusted such that the recombinant GnT-Vb showed a linear increase in the rate of product formation as a function of incubation times up to 240 min or amounts of GnT-Vb (data not shown). GnT-Vb displayed relatively low activity with the trisaccharide acceptor in the absence of divalent cation, and Mn^{2+} clearly stimulated GnT-Vb activity about 4-fold (Figure 2A), by contrast to GnT-Va, which is fully active in EDTA and whose activity actually decreases in the presence of Mn^{2+} (Shoreibah et al. 1992). The same effect of cation was also demonstrated using the transiently expressed enzyme (Kaneko et al. 2003). Optimum Mn^{2+} concentration for GnT-Vb was found to be 10–40 mM; subsequent experiments were performed in the presence of 10 mM Mn^{2+}. Mn^{2+} was the most effective cation for stimulating activity (Figure 2B). The optimal pH for GnT-Vb activity was about 8.0 (Figure 2C), which differed from that of GnT-V, whose optimum was 6.5–7.0 (Shoreibah et al. 1992). In

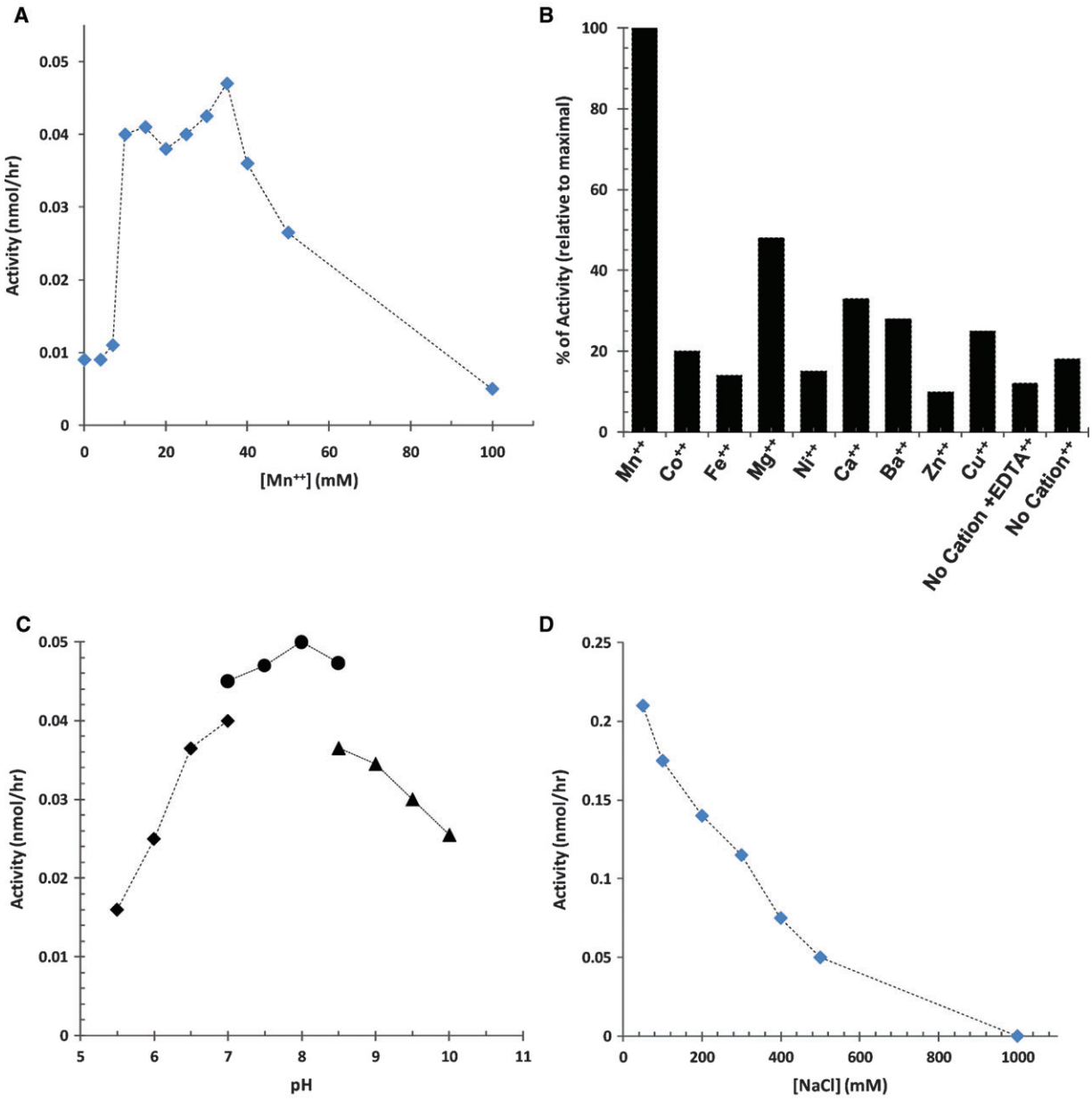

Fig. 2. Effects of different reaction conditions on the activity of GnT-Vb. The activity of nickel-chromatography-purified GnT-Vb was studied under different reactions conditions: (**A**) as a function of Mn^{2+} concentration (0 to 100 mM); (**B**) in the presence of various cations (10 mM of each) or EDTA (100 mM); (**C**) as a function of pH (5.5–10) using three buffered solutions (50 mM MES for pH 5.5 to 7.0; 25 mM HEPES for pH 7 to 8.5; and 100 mM sodium carbonate for pH 8.5 to 10); (**D**) with different concentrations of NaCl (0.025–1 M).

addition, GnT-Vb activity was inhibited by sodium chloride in the assay buffer at concentrations over 50 mM (Figure 2D). The presence of salt does not have the same stabilizing effect for GnT-Vb that was seen with GnT-V, whose activity increases in the presence of NaCl up to 0.2 M before rapidly decreasing (Shoreibah et al. 1992). Secreted, recombinant GnT-V requires a threshold of 0.1 M NaCl, which is required to stabilize its solubility. Decreasing the concentration of NaCl to below 0.1 M causes this recombinant enzyme to precipitate (data not shown).

GnT-Vb displayed typical Michaelis–Menten kinetics with saturation at higher concentrations of UDP-GlcNAc donor and GlcNAcβ1-2Manα1-2Glc-*O*-octyl acceptor (data not shown). Analysis of the UDP-GlcNAc and GlcNAcβ1-2Manα1-2Glc-*O*-octyl reactions yielded apparent K_m values of 0.56 mM and 1.82 mM, respectively (Supplementary Figure 1A, B, Table I). The K_m value of GnT-Vb for the trisaccharide acceptor was about three times higher than that for GnT-V (supplementary Figure 2B, Table I), while the K_m for UDP-GlcNAc was about three times lower than that for GnT-V (Table I). Kinetic analysis of the 2-aminopyridine-labeled asialo-agalacto-biantennary glycan reactions gave a K_m value of 2.30 mM for GnT-Vb (supplementary Figure 1C, Table I), almost 2.5 times higher than that for GnT-V, whose K_m with this acceptor was 0.94 mM (supplementary Figure 2C, Table I).

The reaction of GnT-Vb and the asialo-agalacto-biantennary glycan acceptor was examined in more detail since a previous

Table I. Comparison of Michaelis–Menten constant values measured for GnTVa and GnTVb toward several substrates

	K_m (mM)		V_{max} (nmole/h)		V_{max}/K_m		Relative V_{max}/K_m	
Substrate	GnTVa	GnTVb	GnTVa	GnTVb	GnTVa	GnTVb	GnTVa (%)	GnTVb (%)
UDP-GlcNAc	1.62	0.56	0.070	0.12	0.043	0.214	0.2	16
Octyl	0.53	1.82	11.790	1.09	22.245	0.599	100	44
Asialo-galacto-biantennary	0.94	2.28	19.640	3.10	20.894	1.348	94	100
Benzyl-Man-GlcNAc	0.88	0.61	0.490	0.49	0.557	0.803	3	60
Ac-VEP[GlcNAc(β1,2) Man(α1-)O-T]AV-*NH2*	1.11	0.05	0.004	0.04	0.004	0.880	0.02	65

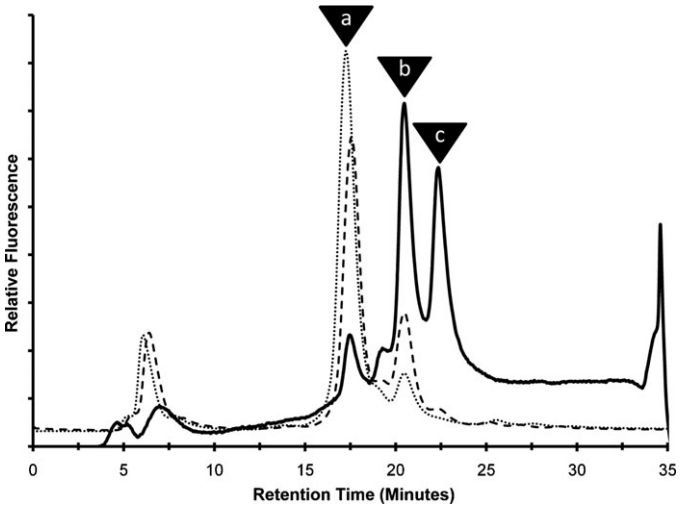

Fig. 3. HPLC separation of reaction products of the fluorescently labeled asialo-agalacto-biantennary glycan substrate after the reaction with GnTVb for various times: (.....), 2 h; (– – –), 8 h; (——), 48 h. Fluorescence of the PA-tagged glycans was detected as described in *Material and methods*. Retention times are indicated for the substrate (Gn_2-bi, peak a), the product with 1 GlcNAc (Gn_3-tri, peak b), and the product with 2 GlcNAc residues (Gn_4-tetra, peak c).

study reported an unusual "double-β(1,6)branched" structure (Inamori et al. 2003) (Scheme I). A time course of reaction, followed by HPLC separation of substrate and products, revealed that after 2 h of reaction between GnT-Vb and the asialo-biantennary structure, a single product eluting at about 20.5 min was observed (Figure 3, peak b). After 8 h of reaction, a second product eluting at about 22 min could begin to be detected (Figure 3, peak c). After 48 h, larger amounts of the second product allowed it to be isolated and further characterized. MALDI-MS analysis (data not shown) suggested that the first product, found in peak b, contained an additional GlcNAc residue compared to the starting material (Figure 3, peak a), while the mass of the secondary product observed after 48 h showed that it contained two additional GlcNAc residues compared to the starting substrate (data not shown). Subsequent NMR structural analysis (Figure 4) revealed that the initial product (peak b) contained an additional GlcNAc linked β1,6- to the α1,6-linked Man, the classic product of the GnT-V reaction. This is reflected in the NMR spectrum by a drastic displacement of the chemical shift signal of the anomeric proton of the Man4′ residue from 4.927 to 4.877 ppm (Figure 4C, Table II) and by the appearance of a signal for the anomeric proton of GlcNAc 7 at 4.545 ppm (Figure 4D, Table II). The secondary product, Figure 3, peak c, observed many hours after the initial rate of the reaction had occurred was shown to contain an GlcNAc linked β1,6- to the α1,6-linked Man and an additional GlcNAc linked β1,6- to the α1,3-linked Man, forming the unusual tetraantennary structure. This was reflected in the NMR spectrum by the appearance of a chemical shift signal for the anomeric proton for the Man 4 residue at 5.078 ppm (Figure 4E, Table II) and a signal for the anomeric proton of GlcNAc 7′ at 4.567 ppm (Figure 4F, Table II). Because of the overlap of peaks b and c encountered during the pooling of fractions for subsequent NMR analysis, peak c also contains some of the triantennary structure found in peak b. These data confirm the structures described in Inamori et al. (2003). Evidence was not found for a product with the unusual triantennary structure where the β1,6 branch occurs on the α1,3-linked Man, which would be predicted to elute in peak b. The synthesis of the "double β1,6-branched" structure, therefore, occurs from branching of the standard triantennary product, but only after a prolonged incubation. Presented with an asialo-agalacto-biantennary substrate, therefore, the product formed by GnT-Vb during the initial rate of reaction is identical to that synthesized by GnT-V, with the unusual "double-β1,6-branched" structure (Scheme I) occurring only after many hours of incubation of GnT-Vb with the substrate.

The apparent K_m values of GnT-Vb and Va were next determined for GlcNAcβ1,2-Man-*O*-benzyl. Man-*O*-benzyl was shown to be an acceptor for POMGnT-I (Zhang et al. 2002); therefore, secreted, recombinant POMGnT-I was used to synthesize the disaccharide acceptor. The K_m values for GnT-Vb and -V for the benzyl-disaccharide acceptor were similar 0.61 and 0.88 mM, respectively (supplementary Figures 1D, 2D, Table I). GnT-Vb had been shown to transfer to a GlcNAc-β1,2-Man-*O*-peptide acceptor (Inamori et al. 2004); therefore, it was of considerable interest to determine the relative K_m values of GnT-Vb and -V toward a glycopeptide known to express GlcNAcβ1,2-Man-*O*-Ser/Thr-. A glycopeptide from α-dystroglycan with the sequence *Ac*-VEP[Man(α1-)*O*-T]AV-*NH2*, known to express this glycan (L. Wells, personal communication), was synthesized, glycosylated using POMGnT-I, and utilized for the kinetic measurements. Supplementary Figures 1E and 2E show the kinetic profiles for both enzymes, which revealed that GnT-Vb displayed an apparent K_m of 0.05 mM toward the peptide compared to 1.1 mM for GnT-V (Table I). These results represent the greatest difference between the two enzymes in K_m values for all substrates tested, over a 20-fold difference, and show a clear distinction between the two enzymes for an *O*-Man-linked glycopeptide acceptor. Interestingly, GnT-V showed little difference in K_m values between the benzyl-disaccharide and glycopeptide, while GnT-Vb showed over a 10-fold difference in K_m values between these substrates, suggesting that the

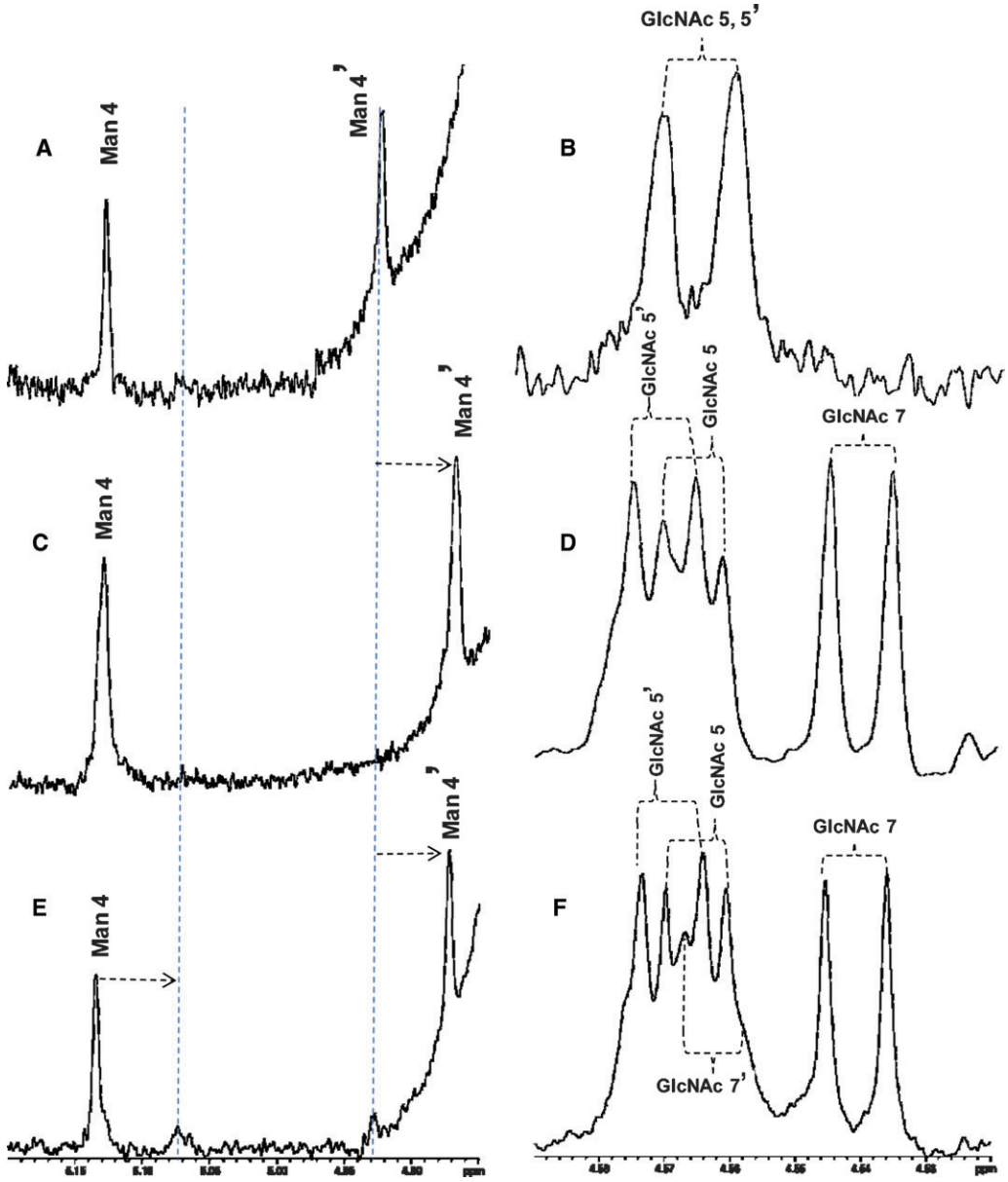

Fig. 4. NMR analysis of GnTVb products. The labeled asialo-agalacto biantennary substrate was reacted with GnT-Vb, the reactions products were separated by HPLC (Figure 3), and fractions collected. The HPLC fractions that contained the unreacted substrate (Gn_2-bi, peak a), the triantennary product with one GlcNAc added (Gn_3-tri, peak b), and the tetraantennary product with two GlcNAc residues added (Gn_4-tetra, peak c) were pooled, dried, and analyzed at 25°C using Varian 800 and 900 MHz Inova NMR spectrometers. Signals from the resulting spectra that correspond to chemical shifts of the anomeric protons are presented for peak a (panels **A** and **B**); peak b (panels **C** and **D**) and peak c (panels **E** and **F**). Chemical shifts of these anomeric signals are summarized in Table II. Panels **A**, **C,** and **E** represent regions of the spectra that show chemical shifts from 4.85–5.20 ppm (anomeric protons of Man 4 and Man 4′ residues), and panels **B**, **D**, and **F** represent regions of the spectra from 4.52–4.59 ppm (anomeric protons of GlcNAc 5, GlcNAc 5′, GlcNAc 7, and GlcNAc 7′ residues). Vertical dashed lines in panels **A**, **C**, and **E** indicate displacements of the chemical shifts of the anomeric protons of residues Man 4 and Man 4′ that resulted from the addition of GlcNAc residues by GnTVb.

Table II. Chemical shifts of the oligosaccharide products separated by HPLC denoted

Oligosaccharide structure[a] (HPLC fraction)	Man 4	Man 4′	GlcNAc5	GlcNAc5′	GlcNAc7	GlcNAc7′
Gn_2-bi (peak a)	5.129	4.927	4.566	4.566		
Gn_3-tri (peak b)	5.135	4.877	4.570	4.572	4.545	
Gn_3-tri (peak c)	5.135	4.877	4.570	4.573	4.545	
Gn_4-tetra (peak c)	5.078[b]					4.567[b]

[a]Denoted in Scheme I.
[b]Weak peak; other resonances for this compound are presumably overlapped with those of the major compound.

peptide component of the glycopeptide may be recognized or accommodated in some way by GnT-Vb during the enzymatic reaction.

In order to obtain an index of the efficiency of GnT-V and GnT-Vb for the different acceptors tested in this study (Burchell et al. 1995), the V_{max}/K_m ratios of each substrate were estimated for these enzymes from the Line Weaver–Burk plots shown in supplementary Figures 1 and 2, and the relative V_{max}/K_m values were calculated relative to the substrate that showed the highest V_{max}/K_m for each ezyme (Table I). GnT-V showed, on average, substantially larger V_{max}/K_m ratios than GnT-Vb. In the case of GnT-V, the substrate for which this enzyme was most efficient was the GlcNAcβ1-2Manα1-2Glc-*O*-octyl acceptor (V_{max}/K_m of 22.25). GnT-Vb was most efficient against the asialo-agalacto-biantennary glycan ($V_{max}/K_m = 1.348$). GnT-V showed very low efficiency against the *O*-Man-linked glycopeptide substrate ($V_{max}/K_m = 0.004$) with a relative V_{max}/K_m that is only 0.02% of the most efficient acceptor. GnT-Vb in contrast showed much larger efficiency against this glycopeptide acceptor ($V_{max}/K_m = 0.88$) with a relative V_{max}/K_m that is 65% of the most efficient substrate. These data indicate that in addition to the higher preference of GnT-Vb for the *O*-Man-linked glycopeptide substrate, the catalytic efficiency is substantially larger than that of GnT-V for this acceptor, indicating that GnT-Vb is much more likely to utilize the *O*-Man glycopeptide substrates than GnT-V.

Discussion

"Genomic paralogy" describes closely linked sets of paralogous genes located on more than one chromosomal segment (Kasahara 1999). An archetypical example of genomic paralogy is provided by the HOX gene clusters and their adjacent regions that are found on human chromosomes 2, 7, 12, and 17 (Ruddle et al. 1994). Interestingly, the human GnT-Vb is located on chromosome 17q25.3, while human GnT-V is located at 2q21, similar to two genomic paralogous regions of the HOX gene cluster. The regulation of the transcription of GnT-V has been studied extensively and is controlled in part by oncogene signaling, notably through the *ras-raf-ets* pathway. The promoter region of GnT-Vb, by contrast, shows no similarity to that of GnT-V, and its expression is unresponsive to ets stimulation (data not shown).

Although the human GnT-Vb amino acid sequence is about 41% identical and 53% similar to that of human GnT-V and the aligned lengths are very similar, there are significant differences in the catalytic activities they encode. GnT-Vb requires divalent cation for full activity toward glycopeptide and synthetic substrates while GnT-V is fully active in EDTA and actually shows lower activity in the presence of 10 mM Mn^{++}. Neither enzyme contains the DXD motif usually associated with cation binding; thus, these sister enzymes most likely contain an amino acid region that can compensate for this motif (Busch et al. 1998; Li et al. 2001). The pH optima for the two enzymes also differ significantly. GnT-Vb shows a significantly higher optimum, similar to other glycosyltransferases expressed in neural tissue, for example, protein *O*-mannosyltransferase 1 (Manya et al. 2004) and ceramide galactosyltransferase (Koul and Jungalwala 1981).

The results comparing K_m values of GnT-Vb toward various acceptors are consistent with and extend the observations by Inamori et al. (2003) that GnT-Vb can synthesize *N*-linked β1,6-branched glycans in vitro. The K_m of GnT-Vb toward the asialo-agalacto-biantennary structure was only 2.5 times that of GnT-V, suggesting that GnT-Vb could possibly function in the synthesis of *N*-linked structures in vivo in cells with no or low GnT-V activity. By contrast, the K_m of GnT-Vb for the peptide-*O*-Man-GlcNAc substrate is over 20 times lower than that for the *N*-linked glycan substrate with a much greater V_{max}/K_m ratio which reflects a substantially greater catalytic efficiency, showing that its preferred substrate by far is the *O*-linked glycopeptide. Strictly based on K_m values comparisons, GnT-V displays K_m values that are relatively similar between the *N*-linked glycan and *O*-linked glycopeptide, suggesting the possibility that it could participate in the synthesis of mannosyl-*O*-linked glycans in vivo. However, the fact that the V_{max}/K_m ratio of GnT-V for the glycopeptide substrate is three orders of magnitude smaller than that of the *N*-linked glycans suggests that GnT-V would poorly glycosylate *O*-Man-linked glycopeptides in vivo. The relative contribution of each of these enzymes to the synthesis of *N*- and *O*-linked glycans in brain tissue and in specific neural cell types has not been studied, but will, of course, be dependent on factors such as their relative levels of expression and compartmentalization in the Golgi apparatus. Further answers to this question await analysis of glycan structures from mice that lack GnT-V and -Vb.

Many glycoprotein substrates are known for GnT-V and range from human erythropoietin (Sasaki et al. 1987) to various growth factor receptors (Partridge et al. 2004; Guo et al. 2007). A substrate for GnT-Vb has recently been identified in neuroblastoma SH-SY5Y cells, the receptor protein tyrosine phosphatase-β (Abbott et al. 2008). Overexpression of GnT-Vb results in an increase in the HNK epitope expression on RPTP-β, detected by the monoclonal antibody, CAT-315, which binds to predominantly *O*-Man-linked HNK structures. A detailed understanding of the glycan structures on RPTP-β and the apparent preference of β1,6-glycan branching of *O*-linked structures by GnT-Vb is clearly necessary. Moreover, changes in the expression of the CAT-315 epitope on RPTP-β, resulting from modulation of GnT-Vb expression levels, caused changes in the phosphatase activity of RPTP-β, measured toward both an exogenous and endogenous substrate. This regulation appeared to stem from differences in the ability of the receptor to dimerize on the cell surface in a galectin-dependent manner. In order to understand the function of GnT-Vb, it is clearly of interest to identify other glycoprotein substrates for GnT-Vb in neural tissue, determine if GnT-Vb glycosylation can also regulate their functions, and compare the relative in vivo substrate preferences of GnT-V and -Vb to determine common and unique glycoprotein substrates for each enzyme.

Material and methods

Materials

All biochemical and chemical reagents were purchased from Sigma Chemical Co (St. Louis, MO). All solvents were HPLC grade and purchased from Fisher Scientific. The other enzymes and reagents obtained from Sigma (Waltham, MA) included 2-aminopyridine, dextran, 2,5-dihydroxybenzoic acid (DHB) and β1,4 galactosyltransferase. Oligonucleotides were purchased from IDT (Coralville, IA). *E. coli* DH5α

cells were purchased from Invitrogen (Carlsbad, CA). The High Pure Plasmid Isolation Kit was purchased from Roche (Indianapolis, IN). The Qiaquick gel extraction kit and Ni^{2+}-nitrilotriacetate (Ni-NTA) resin were purchased from Qiagen (Valencia, CA). All restriction enzymes and T4 DNA ligase were purchased from New England Biolabs (Ipswich, MA). *Spodoptera frugiperda* (Sf9) insect cells and Lec8 CHO cells were purchased from A.T.C.C (Manassas, VA). PEAK^{Stable} Cells (modified HEK-293 cells) and pEAK vector were purchased from EdgeBioSystems (Gaithersburg, MD). pBS with *Trypanosoma cruzi* signal sequence (pBS-SS) was a gift from Dr. Kelley Moremen (University of Georgia, Athens, GA). DMEM, fetal bovine serum, penicillin/streptomycin, and SF9 media were purchased from Mediatech Inc. (Herndon, VA). C18 Sep-Pak cartridges were obtained from Waters (Milford, MA). The TSK-Amide-80 column (4.6 × 250 mm) was purchased from Tosoh Biosciences (Montgomeryville, PA). UDP-[^{3}H]GlcNAc was purchased from American Radiolabeled Chemicals (St. Louis, MO). The synthetic trisaccharide acceptor GlcNAcβ1-2Manα1-2Glc-*O*-octyl was purchased from Chemica Alta (Edmonton, Canada). 2-Aminopyridine (2-AP) labeled asialoagalacto- and asialo-biantennary acceptors were prepared and characterized previously (Kaneko et al. 2003). Man(α1-)*O*-benzyl was purchased from Toronto Research Chemicals Inc. (Toronto, Canada). *Ac*-VEP[Man(α1-)*O*-T]AV-NH_2 was synthesized by the Service Synthesis Laboratory (University of Georgia, Athens, GA). *N*-Acetylglucosaminyltransferase I.2 was a gift from Dr. Harry Schachter (Hospital for Sick Children, Toronto, Canada). A mouse His tag monoclonal antibody was purchased from Novagen (San Diego, CA). Goat anti-mouse IgG was purchased from Santa Cruz Biotechnology Inc. (Santa Cruz, CA). Western Lightning Chemiluminescence Reagent and En^{3}Hance were purchased from PerkinElmer (Boston, MA). BioMax MS film and BioMax Transcreen LE were purchased from Kodak (Rochester, NY).

Construction of a cDNA encoding recombinant soluble human GnT-Vb

The cDNA encoding the truncated forms of GnT-Vb was obtained by PCR using pCD-VB and pCD-VB (Kaneko et al. 2003) as a template. A 2.1 kb fragment encoding the truncated form of GnT-VB and GnT-VB(+) (amino acids 100–782/4, respectively) was amplified by PCR using primers XbaI-F298TVB: 5′-ccatctagaGCAGACAGGATGCCCCCTGG-3′, and hVB-R2385-NotI: 5′-ctcgcggccgcGCTCACAGACAGCCCTGGC ACAAG-3′ (with *Xba*I and *Not*I restriction sites underlined, respectively). PCR conditions were: the PCR products were run on a 1% agarose gel to verify amplification, and the amplified fragments were purified by a gel purification kit (Qiagen). The PCR products were then subcloned into the shuttle vector pCRII-TOPO (Invitrogen), which was amplified, purified, and then digested with *Xba*I and *Not*I. The digested samples were run on a 1% agarose gel, and the inserts were purified as described above. The inserts were then subcloned downstream and in frame of a pBS vector containing an ATG start site, *T. cruzi* signal sequence, and a His tag (pBS-SS-His) using an *Avr*II and *Not*I site. pBS-SS-His-TVB and pBS-SS-His-TVB(+) were then amplified, purified, and digested with *Eco*RI and *Not*I to extract SS-His-TVB (−) and SS-His-TVB(+). The digested samples were run on a 1% agarose gel and the inserts were purified as described above. These inserts were cloned into the pEAK mammalian expression vector using the *Eco*RI and *Not*I cloning sites. At all stages, DNA sequences were verified by sequence analysis.

Cell culture and expression of sshGnT-VB in HEK-293 cells

HEK-293 cells were grown at 37°C with 5% CO_2 in DMEM supplemented with 10% FBS/2 mM L-Gln/100 units/mL penicillin/50 μg/mL streptomycin in T-75 flasks. HEK-293 cells were transfected with 12 μg of pEAK-GnT-VB (−) and TVB(+) using the calcium phosphate method (Chen and Okayama 1987). Once the stable cell line was established according to the protocol prepared by the expression plasmid manufacturer, the cloned cells were maintained in culture media supplemented with 2 μg/mL puromycin. Protein expression with pEAK-GnT-Vb produces a soluble protein containing an N-terminal $(His)_6$ tag. GnT-Vb was partially purified using a 25 mL Ni-NTA fast flow column. GnT-Vb-containing media (500 mL) were centrifuged at 9500 rpm for 30 min to remove any cell debris. The media were then filtered using a 0.2 μm filter and brought up to 25 mM Hepes, pH 8.0, and 50 mM NaCl. The solvents used were buffer A containing 25 mM Hepes, pH 8.0, and 50 mM NaCl and buffer B containing 25 mM Hepes, pH 8.0, 50 mM NaCl, and 300 mM imidazole. The flow rate was maintained at 3 mL/min. After injection of the sample, the column was maintained at 0% B for 300 mL, followed by a linear gradient to 100% B for 300 mL. The column was maintained at 100% B for 150 mL. The column was then washed in 0% B for 100 mL. Fractions containing GnT-Vb were verified by activity assays (described below) and Western blot analysis.

Western blot analysis

The partly purified GnT-Vb was separated by SDS–PAGE (4–20% gel; Biorad) and transferred to a Biotrace PVDF membrane. The membrane was probed with a 1:1000 diluted mouse anti-His antibody. Proteins were visualized by incubation with a 1:10,000 dilution of goat anti-mouse conjugated to horseradish peroxidase followed by staining with a Western Lightning Chemiluminescence Reagent according to manufacturer's protocol.

Assays for GnT-V and Vb

GnT-V assays were performed as described (Chen et al. 1995; Buckhaults et al. 1997). For GnT-Vb, 1.5 mL microcentrifuge tubes (assay tubes) containing 0.4 mM UDP-GlcNAc, 10^6 cpm UDP-[^{3}H]GlcNAc (25 cpm/pmol), 2 mM ADP, and 0.4 mM GlcNAcβ1-2Manα1-2Glc-*O*-octyl acceptor were dried under vacuum. The sample (0.005 mL) was mixed in equal parts to a buffer to give a final concentration of 25 mM HEPES, pH 8.0, 50 mM NaCl, 0.1% Triton X-100, and 10 mM $MnCl_2$ and was incubated in assay tubes for 1 h at 37°C. Kinetic values were obtained for the UDP-GlcNAc donor and several acceptors using reciprocal velocity/substrate plots at different concentrations which are shown in the results section. Assays were carried out at 37°C for times ranging from 1 to 4 h. Radiolabeled products from the GlcNAcβ1-2Manα1-2Glc-*O*-octyl, Man(α1-)*O*-benzyl, and GlcNAc(β1-2)Man(α1-)*O*-benzyl acceptors were purified on SepPak Plus C_{18} cartridges as described (Shoreibah et al. 1993). Fluorescent products from 2-AP asialoagalactobiantennary and 2-AP asialo-agalacto-biantennary acceptors were analyzed by separation on a TSK-Amide column.

Gradient and buffers were used as described (Hase 1994; Kamar et al. 2004). Buffer A: 3% acetic acid/H_2O, pH 7.3 with triethylamine; buffer B: 80% acetonitrile, 3% acetic acid, pH 7.3 with triethylamine. After applying the sample, elution was carried out with a linear gradient from 0% to 10% of A over 2 min at a flow rate of 1 mL/min. This was followed by a linear gradient from 10% to 30% A for 60 min and then 30% to 100% A for 1 min. The column was run isocratically for 10 min, followed by a linear gradient to 0% for 2 min. The column was re-equilibrated in 0% A for 14 min, at which point the next sample was injected. GlcNAc(β1-2)Man(α1-)*O*-benzyl and *Ac*-VEP[GlcNAc(β1,2)Man(α1-)*O*-T]AV-NH_2 were synthesized from their precursors using POMGnTI (Zhang et al. 2002). The synthetic product from the glycosylated peptide acceptor *Ac*-VEP [GlcNAc(β1,2)Man(α1-)*O*-T]AV-NH_2 was purified on a Hypersyl-APS2 column using the following conditions. Buffer A: 50 mM ammonium formate, pH 5; buffer B: 100% acetonitrile. After applying the sample, elution was carried out with a linear gradient from 0% to 23% of B over 30 min at a flow rate of 1 mL/min. This was followed by a linear gradient from 23% to 100% B for 5 min and then maintained at 100% B for 10 min. A linear gradient was run from 100% B to 0% B for 1 min. The column was re-equilibrated in 0% B for 20 min, at which point the next sample was injected. Product was detected by an UV detector then collected and dried. Metal requirements were determined using a 10 mM concentration of bivalent cation and pH optima was determined using $MgCl_2$ instead of $MnCl_2$ due to precipitation of $MnCl_2$ at higher pH values. Assay buffers and conditions were carried out as described above. Concentrations of the GnT-Vb protein were determined by subjecting enzyme preparations to SDS–PAGE, followed by silver staining. Various concentrations of protein standards were run and stained on the same gel. Following densitometric staining, a standard curve was generated and protein concentration of the GnT-Vb band (identified by Western blotting with the anti-His antibody) determined. We have used this methodology to estimate the concentration of GnT-V in preparations (Shoreibah et al. 1992).

NMR product characterization

One hundred nmoles of PA-labeled asialo-agalacto biantennary acceptor was reacted with GnT-Vb as described above and the reaction was incubated for 36 h. The products were then purified by HPLC as described (Kaneko et al. 2003), collected using at automatic fraction collector, and pooled. Purified oligosaccharide fractions were lyophilized from 99% D_2O and then dissolved in 99.96% D_2O. For NMR analysis, data were collected at 25°C on Varian 800 and 900 MHz Inova spectrometers. Chemical shifts were initially referenced to the residual HDO signal set to 4.77 ppm and compared to values reported in Inamori et al. (2003).

Supplementary Data

Supplementary data for this article is available online at http://glycob.oxfordjournals.org/.

Funding

The National Cancer Institute (CA064462).

Acknowledgements

We are grateful to Dr. Mika Kaneko, for insights into glycosyltransferase paralogy, Dr. David Live for synthesis of the synthetic Man-peptide substrate, Dr. John Glushka for performing the NMR analysis. We also wish to thank Dr. Harry Schachter for the cDNA encoding POMGnT-I.

Conflict of interest statement

None declared.

References

Abbott KL, Matthews RT, Pierce M. 2008. Receptor tyrosine phosphatase beta (RPTPbeta) activity and signaling are attenuated by glycosylation and subsequent cell surface galectin-1 binding. *J Biol Chem*. 283:33026–33035.

Buckhaults P, Chen L, Fregien N, Pierce M. 1997. Transcriptional regulation of *N*-acetylglucosaminyltransferase V by the *src* oncogene. *J Biol Chem*. 272:19575–19581.

Burchell B, Brierley CH, Rance D. 1995. Specificity of human UDP-glucuronosyltransferases and xenobiotic glucuronidation. *Life Sci*. 57:1819–1831.

Busch C, Hofmann F, Selzer J, Munro S, Jeckel D, Aktories K. 1998. A common motif of eukaryotic glycosyltransferases is essential for the enzyme activity of large clostridial cytotoxins. *J Biol Chem*. 273:19566–19572.

Chai W, Yuen CT, Kogelberg H, Carruthers RA, Margolis RU, Feizi T, Lawson AM. 1999. High prevalence of 2-mono- and 2,6-di-substituted manol-terminating sequences among *O*-glycans released from brain glycopeptides by reductive alkaline hydrolysis. *Eur J Biochem*. 263:879–888.

Chen C, Okayama H. 1987. High-efficiency transformation of mammalian cells by plasmid DNA. *Mol Cell Biol*. 7:2745–2752.

Chen L, Zhang N, Adler B, Browne J, Freigen N, Pierce M. 1995. Preparation of antisera to recombinant, soluble *N*-acetylglucosaminyltransferase V and its visualization in situ. *Glycoconj J*. 12:813–823.

Endo T. 2005. Aberrant glycosylation of alpha-dystroglycan and congenital muscular dystrophies. *Acta Myol*. 24:64–69.

Endo T, Manya H. 2006. *O*-Mannosylation in mammalian cells. *Methods Mol Biol*. 347:43–56.

Fernandes B, Sagman U, Auger M, Demetrio M, Dennis JW. 1991. Beta 1-6 branched oligosaccharides as a marker of tumor progression in human breast and colon neoplasia. *Cancer Res*. 51:718–723.

Guo HB, Randolph M, Pierce M. 2007. Inhibition of a specific *N*-glycosylation activity results in attenuation of breast carcinoma cell invasiveness-related phenotypes: Inhibition of epidermal growth factor-induced dephosphorylation of focal adhesion kinase. *J Biol Chem*. 282:22150–22162.

Hase S. 1994. High-performance liquid chromatography of pyridylaminated saccharides. *Methods Enzymol*. 230:225–237.

Inamori K, Endo T, Gu J, Matsuo I, Ito Y, Fujii S, Iwasaki H, Narimatsu H, Miyoshi E, Honke K, et al. 2004. *N*-Acetylglucosaminyltransferase IX acts on the GlcNAc beta 1,2-Man alpha 1-Ser/Thr moiety, forming a 2,6-branched structure in brain *O*-mannosyl glycan. *J Biol Chem*. 279:2337–2340.

Inamori K, Endo T, Ide Y, Fujii S, Gu J, Honke K, Taniguchi N. 2003. Molecular cloning and characterization of human GnT-IX, a novel beta1,6-*N*-acetylglucosaminyltransferase that is specifically expressed in the brain. *J Biol Chem*. 278:43102–43109.

Inamori K, Mita S, Gu J, Mizuno-Horikawa Y, Miyoshi E, Dennis JW, Taniguchi N. 2006. Demonstration of the expression and the enzymatic activity of *N*-acetylglucosaminyltransferase IX in the mouse brain. *Biochim Biophys Acta*. 1760:678–684.

Kamar M, Alvarez-Manilla G, Abney T, Azadi P, Kumar Kolli VS, Orlando R, Pierce M. 2004. Analysis of the site-specific *N*-glycosylation of beta1,6 *N*-acetylglucosaminyltransferase V. *Glycobiology*. 14:583–592.

Kaneko M, Alvarez-Manilla G, Kamar M, Lee I, Lee JK, Troupe K, Zhang W, Osawa M, Pierce M. 2003. A novel beta(1,6)-*N*-acetylglucosaminyltransferase V (GnT-VB)(1). *FEBS Lett*. 554:515–519.

Kang R, Saito H, Ihara Y, Miyoshi E, Koyama N, Sheng Y, Taniguchi N. 1996. Transcriptional regulation of the *N*-acetylglucosaminyltransferase V gene in human bile duct carcinoma cells (HuCC-T1) is mediated by Ets-1. *J Biol Chem*. 271:26706–26712.

Kasahara M. 1999. Genome dynamics of the major histocompatibility complex: Insights from genome paralogy. *Immunogenetics*. 50:134–145.

Kim YS, Kang HY, Kim JY, Oh S, Kim CH, Ryu CJ, Miyoshi E, Taniguchi N, Ko JH. 2006. Identification of target proteins of *N*-acetylglucosaminyl transferase V in human colon cancer and implications of protein tyrosine phosphatase kappa in enhanced cancer cell migration. *Proteomics*. 6:1187–1191.

Koul O, Jungalwala FB. 1981. UDP-galactose:ceramide galactosyltransferase of rat central-nervous-system myelin. *Biochem J*. 194:633–637.

Lehle L, Cohen RE, Ballou CE. 1979. Carbohydrate structure of yeast invertase. Demonstration of a form with only core oligosaccharides and a form with completed polysaccharide chains. *J Biol Chem*. 254:12209–12218.

Li J, Rancour DM, Allende ML, Worth CA, Darling DS, Gilbert JB, Menon AK, Young WW Jr. 2001. The DXD motif is required for GM2 synthase activity but is not critical for nucleotide binding. *Glycobiology*. 11:217–229.

Manya H, Chiba A, Yoshida A, Wang X, Chiba Y, Jigami Y, Margolis RU, Endo T. 2004. Demonstration of mammalian protein *O*-mannosyltransferase activity: Coexpression of POMT1 and POMT2 required for enzymatic activity. *Proc Natl Acad Sci USA*. 101:500–505.

Palcic MM, Heerze LD, Pierce M, Hindsgaul O. 1988. The use of hydrophobic synthetic glycosides as acceptors in glycosyltranferase assays. *Glycoconj J*. 5:49–63.

Partridge EA, Le Roy C, Di Guglielmo GM, Pawling J, Cheung P, Granovsky M, Nabi IR, Wrana JL, Dennis JW. 2004. Regulation of cytokine receptors by Golgi *N*-glycan processing and endocytosis. *Science*. 306:120–124.

Ruddle FH, Bentley KL, Murtha MT, Risch N. 1994. Gene loss and gain in the evolution of the vertebrates. *Dev Suppl*, 155–161.

Saito H, Nishikawa A, Gu J, Ihara Y, Soejima H, Wada Y, Sekiya C, Niikawa N, Taniguchi N. 1994. cDNA cloning and chromosomal mapping of human *N*-acetylglucosaminyltransferase V+. *Biochem Biophys Res Commun*. 198:318–327.

Sasaki H, Bothner B, Dell A, Fukuda M. 1987. Carbohydrate structure of erythropoietin expressed in Chinese hamster ovary cells by a human erythropoietin cDNA. *J Biol Chem*. 262:12059–12076.

Schachter H, Vajsar J, Zhang W. 2004. The role of defective glycosylation in congenital muscular dystrophy. *Glycoconj J*. 20:291–300.

Shoreibah M, Hindsgaul O, Pierce M. 1992. Purification and characterization of *N*-acetylglucosaminyltransferase V from rat kidney. *J Biol Chem*. 267:2920–2927.

Shoreibah M, Perng GS, Adler B, Weinstein J, Basu R, Cupples R, Wen D, Browne JK, Buckhaults P, Fregien N, et al. 1993. Isolation, characterization, and expression of a cDNA encoding *N*-acetylglucosaminyltransferase V. *J Biol Chem*. 268:15381–15385.

Warren CE, Krizus A, Roy PJ, Culotti JG, Dennis JW. 2002. The *Caenorhabditis elegans* gene, gly-2, can rescue the *N*-acetylglucosaminyltransferase V mutation of Lec4 cells. *J Biol Chem*. 277:22829–22838.

Yuen CT, Chai W, Loveless RW, Lawson AM, Margolis RU, Feizi T. 1997. Brain contains HNK-1 immunoreactive *O*-glycans of the sulfoglucuronyl lactosamine series that terminate in 2-linked or 2,6-linked hexose (mannose). *J Biol Chem*. 272:8924–8931.

Zhang W, Betel D, Schachter H. 2002. Cloning and expression of a novel UDP-GlcNAc:alpha-D-mannoside beta1,2-*N*-acetylglucosaminyltransferase homologous to UDP-GlcNAc:alpha-3-D-mannoside beta1,2-*N*-acetylglucosaminyltransferase I. *Biochem J*. 361:153–162.

Zhao Y, Sato Y, Isaji T, Fukuda T, Matsumoto A, Miyoshi E, Gu J, Taniguchi N. 2008. Branched *N*-glycans regulate the biological functions of integrins and cadherins. *FEBS J*. 275:1939–1948.

Zhao YY, Takahashi M, Gu JG, Miyoshi E, Matsumoto A, Kitazume S, Taniguchi N. 2008. Functional roles of *N*-glycans in cell signaling and cell adhesion in cancer. *Cancer Sci*. 99:1304–1310.